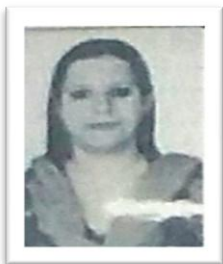


Inner- and Outer-Shell Electron Dynamics in $H^+ + Na(3s)$ Collisions



Vidhu Khullar
Assistant Professor,
Deptt. of Physics,
A.S. College, Khanna



Sanjay Bector
Assistant Professor,
Deptt. of Physics,
G.N.G. College,
Ludhiana

Abstract

In this paper a detailed study of keV $H^+ + Na$ collisions is presented. The MOTRIMS experiments confirm that capture of the outer-shell $3s$ electron dominates at low energy. But for higher energies they present the first direct evidence of charge transfer being dominated by capture of a $2p$ inner-shell electron instead of outer-shell capture. With this observation one-electron capture can be seen as a result of two distinct processes. At low energies, $E < 10$ keV/amu, it is dominated by outer-shell capture into $H(n=2)$, while at high energies, $E > 40$ keV/amu, inner-shell capture from the $2p$ -shell into $H(n=1)$ is the main process, i.e. already at energies lower than expected from the "velocity matching" argument.

In the Na^+ recoil spectra two inner-shell capture processes could be identified, namely ISC leaving the outer-shell electron in the $3s$ state or exciting it to $3p$. The relative intensities of these processes revealed the prominent role of multi-electron dynamics in low energy inner-shell capture and a transition to ISC without active outer-shell participation occurring at $\sim 1.4 v_{orb}$ of the outer-shell electron. Inner-shell capture leading to Na^+ recoils has larger cross sections than that of Na^{2+} production, the latter being dominated by transfer ionization. Good overall agreement between our MOTRIMS data and the TC-BGM calculations has been found.

Keywords: ADC Autoionizing Double Capture, AO Atomic Orbital, AOM Acousto-Optical Modulator, BGM Basis Generator Method, CBM Classical Over-Barrier Model, CCD Charge Coupled Device, CDC Correlated-Double-Capture, COLTRIMS Cold Target Recoil-Ion Momentum Spectroscopy CTE Correlated Transfer And Excitation, CTMC Classical Trajectory Monte Carlo, DC Double Capture, DCS Differential Cross Section, DCSI Double Capture And Single Ionization, DI Double Ionization, ECC Electron Capture Into The Continuum, ECRIS Electron Cyclotron Resonance Ion Source, EEC Electron Excitation Into The Continuum, EOM Electron-Optical Modulator, FSR Free Spectral Range, FWHM Full Width Half Maximum, ISC Inner-Shell Capture, ISDC Inner-Shell Double Capture, LZ Landau-Zener, MOT Magneto-Optical Trap, MOTRIMS Magneto-Optical Trap Recoil-Ion Momentum Spectroscopy, OSC Outer-Shell Capture, PES Photon Emission Spectroscopy, PZT Piezoelectric Translator.

Introduction

Collisions between protons and alkali atoms have been studied extensively in the past. In 1964 Donnally et al. [178] reported first measurements on cross sections for the production of metastable $H(2s)$ in $H^+ + Cs$ collisions. The study of this charge exchange reaction was motivated by the development of spin polarized ion sources. The choice for an alkali target over the earlier proposed molecular hydrogen target as donor to feed the $H(2s)$ channel [179] was taken because for alkalis the ionization energies are lower and the energy defects with the $H(2s)$ state smaller. This leads to larger cross sections which maximize at lower impact energies. The latter facilitates the separation of the metastable hydrogen atoms from the beam of protons by electric or magnetic fields. Soon after, charge exchange on alkalis was proposed to be the first step in the production of polarized negative hydrogen ions [180]. From the 1970's on the motivation to study collisions between protons and alkali atoms shifted towards fusion research (see e.g. [181,182]).

From a theoretical perspective, an appealing feature of ion-alkali-atom collision systems is the shell structure of the alkalis, i.e., a single valence electron outside closed inner shells. It suggests the applicability of quasi-one-electron models in which the dynamics of the loosely bound

outermost electron is governed by the joint Coulomb potential of projectile and target nuclei and an effective potential due to "frozen" inner-shell electrons. Ion-alkali-atom collisions have been valuable test beds for advancing methods to solve the one-electron time-dependent Schrodinger equation because true one-electron systems, i.e., collisions of bare ions on atomic hydrogen, are difficult to handle and control experimentally. Almost all reported quantum mechanical and classical calculations concerning alkali-atom targets rely on the one-electron approximation.

For the $H^+Na(3s)$ collision system, measurements of total cross sections for one-electron capture in the low keV/amu impact energy range are manifold [183-185]. At higher impact energies, also cross sections for two-electron removal were obtained [13,186]. These studies.

| | final states | Q-value (eV) |
|----------------------|----------------------------|--------------|
| OSC | $H(n=1)+Na^+(2p^6)$ | -8.46 |
| | $H(n=2)+Na^+(2p^6)$ | 1.74 |
| | $H(n=3)+Na^+(2p^6)$ | 3.63 |
| | $H^++Na^+(2p^6)+e^-$ | ≥ 5.14 |
| ISC into $n=1$ | $H(n=1)+Na^+(2p^5 3s)$ | 24.5 |
| | $H(n=1)+Na^+(2p^5 3p)$ | 28.7 |
| | $H(n=1)+Na^+(2p^5 3d)$ | 32.5 |
| | $H(n=1)+Na^+(2p^5 4s)$ | 32.7 |
| | $H(n=1)+Na^{2+}(2p^5)+e^-$ | ≥ 38 |
| ISC into $n=2$ | $H(n=2)+Na^+(2p^5 3s)$ | 34.7 |
| | $H(n=2)+Na^+(2p^5 3p)$ | 38.9 |
| | $H(n=2)+Na^+(2p^5 3d)$ | 42.7 |
| | $H(n=2)+Na^+(2p^5 4s)$ | 42.9 |
| | $H^++Na^{2+}(2p^5)+2e^-$ | ≥ 52.3 |

Figure 5.1: Q-value spectrum of Na^+ recoils ions after p-Na collisions at 14 keV/amu. Main contributions come from outer-shell capture (OSC), of which capture into $H(1s)$ and $H(n=2)$ are indicated. Outer-shell ionization starts beyond $Q = 5.14$ eV. On top of the ionization tail the inner-shell capture (ISC) contributions appear. Clearly visible are the two contributions from ISC into $H(1s)$ in combination with $Na^+(2p^5 3s)$ and $Na^+(2p^5 3p)$ as final state. The line through the data is drawn to guide the eye.

These experimental studies were followed and inspired by theoretical progress in coupled channel calculations, using molecular [192-194] or two-center atomic basis set expansions [195-197]. Most recent theoretical work on charge transfer in keV $H^+Na(3s)$ collisions is based on two-center 36 atomic orbital expansion (TCA036) [198], two-center 70-state Sturmian-pseudostate expansion (TCSA070) [199] and classical trajectory Monte Carlo (CTMC) calculations [90].

These one-electron models have been employed with some success. However, the theoretical calculations typically showed a much steeper decrease of the cross section towards higher impact

energies than experimentally observed. The cross sections even seem to flatten out, The necessity to improve the models became apparent already some twenty years ago, when measurements of multiple-electron removal from lithium and sodium atoms by proton.

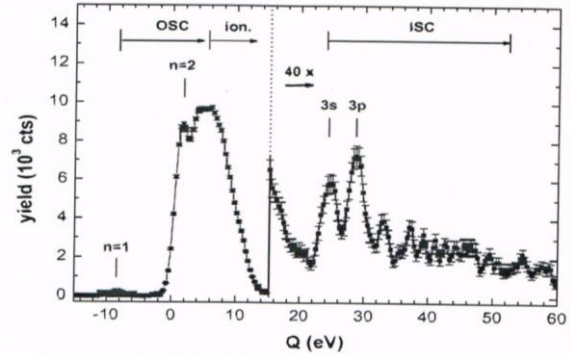


Table 5.1: Q-values of relevant final states after one-electron capture processes in $H^+Na(3s)$ collisions, grouped in either OSC or ISC. Also the Q-values related with the onset of single ionization, transfer ionization and double ionization are given.

Here electron capture and ionization processes in $H^+Na(3s)$ collisions have been studied in the energy range of 4-25 keV/amu. Cross sections for capture and ionization, as well as state selective and differential cross sections for outer-shell capture (OSC) into the $n=1$, $n=2$, and $n=3$ shells of hydrogen have been obtained. Besides charge transfer processes involving the outer-shell electron of Na, also inner-shell capture (ISC) processes have been observed. Note that while OSC in this collision system has been studied extensively, direct identification of pure ISC has not been reported so far.

To introduce this collision system a Q-value spectrum of Na^+ recoils is shown in figure 5.1. Several processes can be recognized in this spectrum. In the OSC part of the spectrum ($Q < I$, where $I = 5.14$ eV is the ionization potential of Na) one can distinguish the contributions of OSC into $H(1s)$ ($Q = -8.46$ eV) and $H(n=2)$ ($Q = +1.74$ eV) which is the main capture channel. Capture into higher n states cannot be resolved. Ionization of the outer-shell electron leads to $Q > I$. On top of the ionization tail the ISC contribution from the $2p$ shell is found. Although ionization and ISC can have the same Q-value, the latter can be recognized because it gives rise to capture peaks on top of the continuous ionization spectrum. The two main peaks in this part of the Q-value spectrum arise when an inner-shell $2p$ electron is captured into $H(1s)$ and the target is left in either an excited $Na^+(2p^5 3s)$ or $Na^+(2p^5 3p)$ state. The smaller peaks are not identified unambiguously, but are related to more highly excited Na^+ states or ISC into excited hydrogen, $H(n \geq 2)$. The Q-values of the relevant OSC and ISC channels are given in table 5.1. The maximum Q-value for ISC is $Q = 52.3$ eV and occurs when the outer-electron is just excited to the continuum of the target and the inner-shell electron is captured into the continuum of the projectile.

To summarize the processes under investigation, we distinguish between processes in

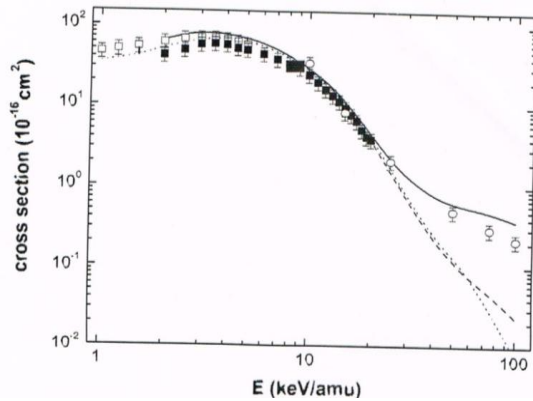
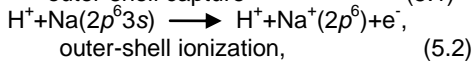
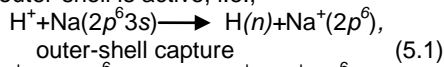
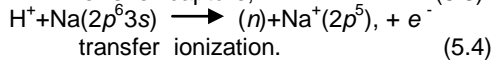
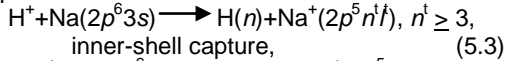


Figure 5.2.: TC-BGM results for total capture (—), and for OSC capture (---); TCSAO70[199] (...). which only the outer-shell is active, i.e.,

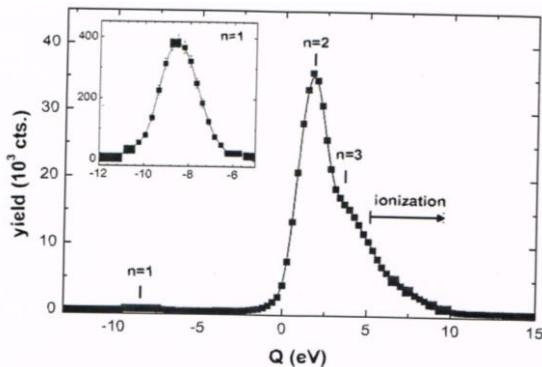


and processes in which also the 2/?-shell contributes,



The experimental results are presented in conjunction with recent TC-BGM calculations. The general features of this close coupling scheme are discussed in section 2.5.1. For the $\text{H}^+ + \text{Na}(3s)$ collision system the basis included the undisturbed states $\psi_i(r)$ of the Na target ($n = 2 - 4$ shells, 19 states) and of the projectile ($n = 1 - 5$ shells, 35 states), as well as 49 pseudostates from the set $\{ \psi_\nu(r, t), \nu \geq 1, \nu \leq V_i \}$ up to order $\nu = 6$, in which V_i is the finite set of target states. A set of 26 impact parameters in the range 0.22 a.u. $b \leq 30$ a.u. was used, while the integrations have been restricted to impact parameters $b \leq 5$ a.u. for the inner electrons. Physically this restriction is fully justified, since the inner-shell electrons are tightly bound.

Figure 5.2 summarizes the total cross sections for one-electron capture. Previous experiments [183-185] and theoretical calculations [197,199] are in very good agreement for low energy, but above 40 keV/amu discrepancies are found. Compared with the measurements of DuBois [13] theory underestimates one-electron capture by up to an order of magnitude. The TC-BGM calculations for total capture, including also the 2s- and 2p-shell, follow the



Remarking

Vol-II * Issue- X* March- 2016

Figure 5.3: Q-value spectrum of Na^+ recoils for 8 keV/amu $\text{H}^+ + \text{Na}(3s)$ collisions. The dominant channel at $Q = +1.74$ eV is capture into $\text{H}(n = 2)$. For $Q > 5.14$ eV the spectrum contains the Na^+ recoils produced by ionization. The inset shows a close-up of the weak $\text{H}(n = 1)$ capture channel. Lines are drawn to guide the eye.

Experimental cross sections, while the pure OSC results are in agreement with previous calculations. From these observations one can already conclude that the high energy behavior of the cross sections is due to the participation of inner-shell electrons.

Aim of the Study

In this paper an extensive MOTRIMS study of electron capture and ionization processes in collisions of H^+ , He^{2+} , C^{6+} and O^{6+} projectile ions on ground state $\text{Na}(3s)$ and laser excited $\text{Na}^*(3p)$ is presented. The investigated energy range of 1 - 25 keV/amu covers the transition from pure electron capture to ionization dominated interactions. The experimental data are presented in conjunction with state-of-the-art theoretical calculations. Classical trajectory Monte Carlo calculations have been carried out by Ron Olson (Rolla, USA). Close-coupling two-center basis generator method calculations were performed by Matthias Keim and Hans Jurgen Liidde (Frankfurt, Germany) and Myroslav Zapukhlyak and Tom Kirchner (Clausthal, Germany). In this paper the results are presented for the collision systems of $\text{H}^+ + \text{Na}(3s)$. In all our findings on (multi-)electron capture are compiled and compared to identify general trends. For single ionization a similar approach is presented.

Outer-Shell Processes

First the pure outer-shell processes, i.e. single outer-shell capture or ionization will be considered. In the Q-value spectra these processes appear at $Q < 24.5$ eV. A typical Q-value spectrum of Na^+ recoils resulting from 8 keV/amu $\text{H}^+ + \text{Na}(3s)$ collisions is shown in figure 5.3. The energy dependence of pure outer-shell processes is illustrated in figure 5.4. Two effects can be seen directly. First of all the state selectivity is lost with increasing collision energy. At 4 keV/amu 85% of the intensity is due to capture into the $\text{H}(w = 2)$ shell, while at 10 keV/amu ionization is equally strong as this channel. Above 16 keV/amu capture into higher shells is equally probable as capture into $n = 2$. Secondly, the ionization distribution is shifted towards higher Q-values. One can show that the Q-values of ionization processes are directly connected to the energy of the emitted electrons in the projectile frame (see appendix C). At low projectile energy most of the emitted electrons are projectile centered (electron capture into the continuum), thus having very low energy in the projectile frame. But with increasing projectile velocity, ionized electrons strand in between the target and the projectile. At $E = 25$ keV/amu target centered electrons would correspond to an energy of 13.6 eV in the projectile frame, appearing at $Q = 18.7$ eV (see chapter 10 for a general discussion on single.

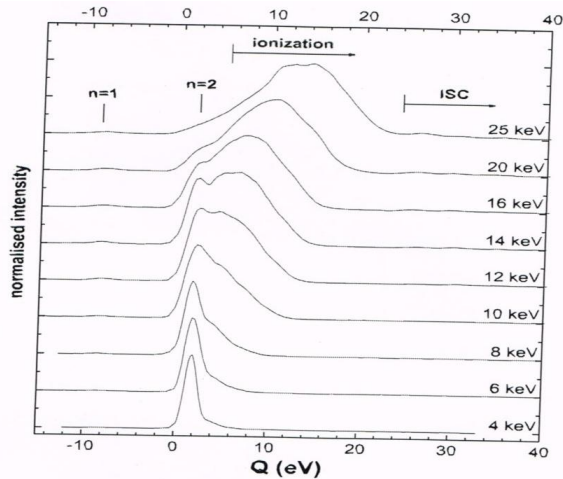


Figure 5.4: Compilation of Q-value spectra of Na⁺ recoils resulting from H⁺+Na(3s) collisions. The positions of capture into H(n=1) and H(n=2) are indicated, as well as the onsets for ionization and inner-shell capture (ISC).

Inner-Shell Processes

A first indication of the participation of inner-shell electrons in ion-atom collisions was found in the high-energy behavior of the total capture cross section (see e.g. [203] and references therein). The flattening out of the total cross section instead of a rapid decrease was explained by an increased participation of core electrons. At higher energies the incident ion's velocity approaches that of the core electrons. In general, the capture cross section is expected to maximize if there is "velocity matching" between the target electron and the projectile. Total one-electron capture cross sections for the H⁺+Na(3s) collisions also exhibit this trend (see figure 5.2).

A RIMS technique enables the direct observation of (sub-) shell-specific processes, as the Q-value of a specific reaction can be determined. Previously, this level of detail was accessible only indirectly via spectroscopy of Auger electrons or photons, which are charac-

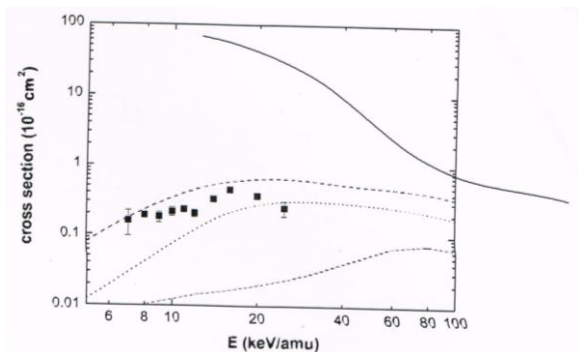


Figure 5.5: Inner shell capture cross sections for H⁺+Na collisions as functions of impact energy. Present experiment; ISC from 2p-shell Theory: TC-BGM results for total one-electron capture ¹⁰(-), ^{10,10}_{osc}(- -); Multinomial ISC from 2p-shell (...) and ISC from 2s-shell (- -). As stated above, inner-shell processes involving alkalis have not been

reported before, because capture from the uppermost inner-shell cannot lead to Auger decay. Only radiative decay is possible. Outer- and inner-shell capture processes appear both in the Na⁺ recoil spectrum, but as shown in figure 5.1 they can be distinguished and the assignment is unambiguous. The final states in hydrogen span an energy range of 13.6 eV, while the difference in binding energy of the Na 3s electron and the nearest inner-shell 2p electron is 28 eV.

In the following sections processes in H⁺+Na(3s) collisions involving the 2p-shell are presented. First the pure inner-shell capture contribution in the Na⁺ recoil spectra is discussed. Next, results on transfer ionization are given and compared with pure inner-shell capture.

Inner-Shell One-Electron Capture

From the assignment of the ISC part of the Na⁺ recoil spectrum (see figure 5.1) it is clear that most of its contribution is related to capture into the hydrogen ground state. Therefore in the following inner-shell capture is specified for the processes

$$H^+ + Na(2p^6 3s) \rightarrow H(1s) + Na^+(2p^5 nl), n \geq 3 \quad (5.5)$$

One of the 2p inner-shell electrons is captured into the hydrogen ground state while the outer-shell 3s electron remains bound to the target. In the rest of the discussion the term ISC is used for processes given by equation 5.5.

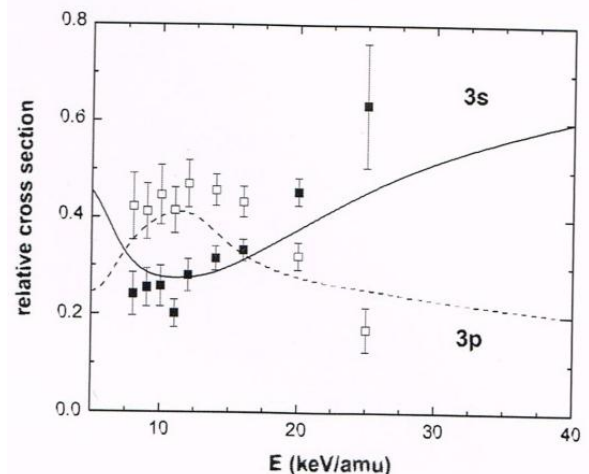


Figure 5.6: MOTRIMS and TC-BGM results for the different contributions to ISC into H(n=1): Na⁺(2p⁵3s) and Na⁺(2p⁵3p) (O, —).

The experimental ISC cross sections obtained are shown in figure 5.6 together with the TC-BGM calculations, in which the total ISC contribution is obtained from the difference between total one-electron capture (¹⁰) and outer-shell capture (¹⁰_{osc}).

Clearly, the dominant contribution to ISC is due to the Na(2p) electrons. The MOTRIMS results agree very well with the calculations. However, this agreement may be somewhat fortuitous, since the calculations are not restricted to the final states probed by the experiments. The experimental ISC excludes the possibility that more than one electron is removed. The Q-value spectra are taken for Na⁺ recoil ions and do not include Na²⁺ recoils. This situation is not respected by taking the difference of net- and single-electron transfer cross sections, but can be modelled by multinomial statistics [72]. The result of

such an analysis is shown figure 5.6. This multinomial ISC is somewhat lower than the difference of net- and single-particle cross sections, which is a direct consequence of the condition that the other electrons - in particular Na(3s) - remain bound to the target.

The two main ISC peaks in the Q-value spectrum (figure 5.1) are due to capture into H(b) leaving the excited Na⁺ recoil in either a 2p⁵3s or 2p⁵3p state. Their relative contributions are shown in figure 5.12. These two channels contribute about 75% of the total ISC. The other 25% can be ascribed to the formation of higher 2p⁵nl states. The main trends in the MOTRIMS data are supported by the calculations: 2p⁵3p gives the largest contribution below E = 18 keV, and 2p⁵3s dominates at higher energies. Below E = 6 keV/amu theory shows again a dominance of 2p⁵3s, which is not supported by the measurements.

To understand a dominance of the 2p⁵3p final state at low energy the following explanation is proposed. This final state implies that the capture of one inner-shell 1p electron is accompanied by the excitation of the outer-shell 3s electron to the 3p orbit, i.e. an active role of the outer-shell electron. In this process the two active electrons form a system with total

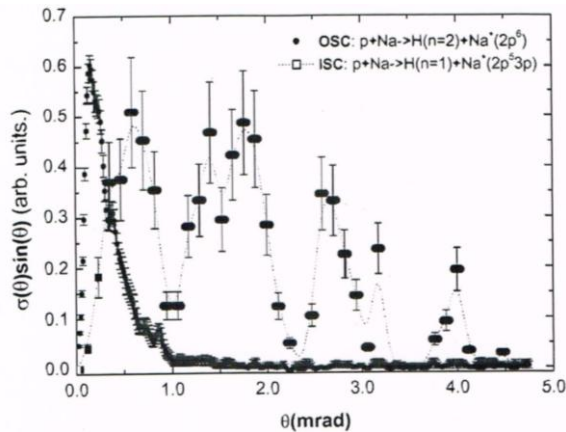


Figure 5.7: Reduced DCS of OSC into H($n=2$) and ISC into H(1s) leading to Na⁺(2p⁵3p) at 14 keV/amu collision energy. In order to compare these processes, in both cases the integral over is normalized. The line is to guide the eye.

Angular momentum $Z = 1$. Because the 2p electron is captured into a 1s state, the outer-shell 3s electron has to change to a p orbital in order to conserve angular momentum. The energetically most favorable p state is the 3p state. This mechanism will only hold if the transition time from the quasi-molecular state to the final state is long enough such that the outer-shell 3s electron can interact with the captured 2p electron. That might be the reason that this channel decreases at higher collision energy.

The energy dependence of the 2p⁵3s population suggests that with increasing projectile velocity the 3s electron does not change its initial orbital and becomes more of a spectator. In fact this is a situation typically assumed in high energy ISC, i.e., charge transfer from different shells can be treated independently (see e.g. [208]). The present data clearly show the transition between ISC with and without outer-shell participation. The transition occurs at about 1.4 V_{orb} of the outer-shell electron, i.e. at

much lower velocity than V_{orb} of the 2p electron (which corresponds to a collision energy of 90 keV/amu).

Objectives

In this paper an extensive MOTRIMS study of electron capture and ionization processes in collisions of H⁺, He²⁺, C⁶⁺ and O⁶⁺ projectile ions on ground state Na(3s) and laser excited Na⁺(3p) is presented. The investigated energy range of 1 - 25 keV/amu covers the transition from pure electron capture to ionization dominated interactions. The experimental data are presented in conjunction with state-of-the-art theoretical calculations. Classical trajectory Monte Carlo calculations have been carried out by Ron Olson (Rolla, USA). Close-coupling two-center basis generator method calculations were performed by Matthias Keim and Hans Jürgen Liidde (Frankfurt, Germany) and Myroslav Zapukhlyak and Tom Kirchner (Clausthal, Germany). In this paper the results are presented for the collision systems of H⁺+Na(3s). In all our findings on (multi-)electron capture are compiled and compared to identify general trends. For single ionization a similar approach is presented.

Conclusion

In this paper a detailed study of keV H⁺+Na collisions is presented. The MOTRIMS experiments confirm that capture of the outer-shell 3s electron dominates at low energy. But for higher energies they present the first direct evidence of charge transfer being dominated by capture of a 2p inner-shell electron instead of outer-shell capture. With this observation one-electron capture can be seen as a result of two distinct processes. At low energies, $E < 10$ keV/amu, it is dominated by outer-shell capture into H($n=2$), while at high energies, $E > 40$ keV/amu, inner-shell capture from the 2p-shell into H($n=1$) is the main process, i.e. already at energies lower than expected from the "velocity matching" argument.

In the Na⁺ recoil spectra two inner-shell capture processes could be identified, namely ISC leaving the outer-shell electron in the 3s state or exciting it to 3p. The relative intensities of these processes revealed the prominent role of multi-electron dynamics in low energy inner-shell capture and a transition to ISC without active outer-shell participation occurring at $\sim 1.4 V_{orb}$ of the outer-shell electron. Inner-shell capture leading to Na⁺ recoils has larger cross sections than that of Na²⁺ production, the latter being dominated by transfer ionization. Good overall agreement between our MOTRIMS data and the TC-BGM calculations has been found.

References

1. R. C. Isler and E. C. Crume, Phys. Rev. Lett. 41, 1296 (1978).
2. J. E. Rice, E. S. Mannar, J. L. Terry, E. Kallne, and J. Kallne, Phys. Rev. Lett. 56, 50 (1986).
3. E. Wolfrum, F. Aumayr, D. Wutte, HP. Winter, E. Hintz, D. Rusboldt, and R. P. Schom, Rev. Sci. Instr. 64, 2285 (1993).
4. M. G. O'Mullane, M. Mattioli, R. Giannella, I. H. Coffey, and N. J. Peacock, Plasma Phys. Control. Fusion 41, 105 (1999).
5. M. von Hellermann, Plasma Phys. Control. Fusion 35, 799 (1993).
6. R. Hoekstra, D. Bodewits, S. Knoop, R. Morgenstem, L. Mendez, L. F. Errea, C. Illasas,

- A. Macias, B. Pons, A. Riera, F. Aumayr, and HP. Winter, Atomic and Plasma-Material Interaction Data for Fusion (in press).
7. C. M. Lisse, K. Denneri, J. Englhauser, M. Harden, F. E. Marshall, M. J. Mumma, R. Petre, J. P. Pye, M. J. Ricketts, J. Schmitt, J. Trumper, and R. G. West, *Science* 274, 205(1996).
 8. T. E. Cravens, *Geophys. Res. Lett.* 24,105 (1997).
 9. P. Belersdorfer, C. M. Lisse, R. E. Olson, G. V. Brown, and H. Chen, *ApJ.* 549, L147 (2001).
 10. D. Bodewits, Z. Juhasz, R. Hoekstra, and A. G. G. M. Tielens, *ApJ.* 606, L81 (2004).
 11. J. de Vries, R. Hoekstra, R. Morgenstem, and T. Schlatholter, *Phys. Rev. Lett.* 91, 053401 (2003).
 12. T. Schlatholter, R. Hoekstra, and R. Morgenstem, *Int. J. Mass Spec.* 233,173 (2004).
 13. R. D. Dubois, *Phys. Rev. A* 34,2738 (1986).
 14. R. Shingal, C. J. Noble, and B. H. Bransden, *J. Phys. B: At. Mol. Opt. Phys.* 20, 793 (1987).
 15. A. R. Schlatmann, R. Hoekstra, H. O. Folkerts, and R. Morgenstem, *J. Phys. B: At. Mol. Opt. Phys.* 25, 3155 (1992).
 16. Y. Dehong, L. Jiarui, L. Ziming, Y. Feng, P. Guangyan, W. Duanwei, and S. Shiang, *Phys. Rev. A* 15, 2931(1989).
 17. A. Jain and T. G. Winter, *J. Phys. B: At. Mol. Opt. Phys.* 29,4675 (1996). [18] W. Fritsch and C. D. Lin, *Phys. Rep.* 202,1 (1991).
 18. S. Y. Ovchinnikov, G. N. Ogurtsov, J. H. Macek, and Y. S. Gordeev, *Phys. Rep.* 389, 119(2004).
 19. E. L. Raab, M. Prentiss, A. Cable, S. Chu, and D. E. Pritchard, *Phys. Rev. Lett.* 59, 2631(1987).
 20. M. H. Anderson, J. R. Ensher, M. R. Matthews, C. E. Wieman, and E. A. Cornell, *Science* 269, 198 (1995).
 21. K. B. Davis, M. O. Mewes, M. R. Andrews, N. J. van Druten, D. S. Durfee, D. M. Kum, and W. Ketterle, *Phys. Rev. Lett.* 75, 3969 (1995).
 22. J. Ullrich, R. Moshhammer, A. Dom, R. Domer, L. P. H. Schmidt, and H. Schmidt-Bocking, *Rep. Prog. Phys.* 66, 1463 (2003).
 23. M. van der Poel, C. V. Nielsen, M. A. Gearba, and N. Andersen, *Phys. Rev. Lett.* 87, 123201 (2001).
 24. X. Flechard, H. Nguyen, E. Wells, I. B. Itzhak, and B. D. DePaola, *Phys. Rev. Lett.* 87, 123203(2001).
 25. J. W. Turkstra, R. Hoekstra, S. Knoop, D. Meyer, R. Morgenstem, and R. E. Olson, *Phys. Rev. Lett.* 87, 123202 (2001).
 26. X. Flechard, H. Nguyen, R. Bredy, S. R. Lundeen, M. Stauffer, H. A. Camp, C. W. Fehrenbach, and B. D. DePaola, *Phys. Rev. Lett.* 91, 243005 (2003).
 27. J. R. Oppenheimer, *Phys. Rev.* 31, 349 (1928).
 28. H. C. Brinkman and H. A. Kramers, *Proc. Acad. Sci. Amsterdam* 33,973 (1930).
 29. H. S. W. Massey and R. A. Smith, *Proc. R. Soc.* 142,142 (1933).
 30. B. H. Bransden and M. R. C. McDowell, *Charge Exchange and the Theory of Ion-Atom Collisions*, Clarendon Press, Oxford, 1992.
 31. L. H. Thomas, *Proc. Roy. Soc.* 114, 561 (1927).
 32. E. Horsdal-Pedersen, C. L. Cocke, and M. Stockli, *Phys. Rev. Lett.* 50, 1910 (1983).
 33. H. Vogt, R. Schuch, E. Justiniano, M. Schuiz, and W. Schwab, *Phys. Rev. Lett.* 57, 2256(1986).
 34. N. Bohr and J. Lindhard, *K. Dan. Vidensk. Selsk. Mat. Fys. Medd.* 28, 1 (1954).
 35. H. Knudsen, H. K. Haugen, and P. Hvelplund, *Phys. Rev. A* 23, 597 (1981).
 36. H. Ryufuku, K. Sasaki, and T. Watanabe, *Phys. Rev. A* 21, 745 (1980).
 37. R. Mann, F. Folkmann, and H. F. Beyer, *J. Phys. B: At. Mol. Opt. Phys.* 14, 1161 (1981).
 38. A. Barany, G. Astner, H. Cederquist, H. Danared, S. Hultdt, P. Hvelplund, A. Johnson, H. Knudsen, L. Liljeby, and K. G. Rensfeld, *Nucl. Instr. Methods B* 9, 397 (1985).
 39. A. Niehaus, *J. Phys. B: At. Mol. Opt. Phys.* 19, 2925 (1986).
 40. H. S. W. Massey, *Rep. Prog. Phys.* 12,248 (1948).
 41. Y. N. Demkov, *Sov. Phys. - JETP* 18,138 (1964).
 42. R. E. Olson, *Phys. Rev. A* 6, 1822 (1972).
 43. R. E. Olson, F. T. Smith, and E. Bauer, *Appl. Opt.* 10, 1848 (1971).
 44. R. Shingal, C. J. Noble, B. H. Bransden, and D. R. Flower, *J. Phys. B: At. Mol. Opt. Phys.* 19, 3951(1986).
 45. L. D. Landau, *Phys. Z. Sow.* 1, 46 (1932).
 46. C. Zener, *Proc. R. Soc.* 137, 696 (1932).
 47. R. E. Olson and A. Salop, *Phys. Rev. A* 14, 579 (1976).
 48. M. Kimura, T. Iwai, Y. Kaneko, N. Kobayashi, A. Matsumoto, S. Ohtani, K. Okuno, S.-Takagi, H. Tawara, and S. Tsurubuchi, *J. Phys. Soc. Japan* 53,2224 (1984).
 49. R. K. Janev and H. Winter, *Phys. Rep.* 117,265 (1985).
 50. K. Taulbjerg, *J. Phys. B: At. Mol. Opt. Phys.* 19, L367 (1986).
 51. J. Schweinzer and H. Winter, *J. Phys. B: At. Mol. Opt. Phys.* 23,3881 (1990).
 52. N. Bohr, *K. Dan. Vidensk. Selsk. Mat. Fys. Medd.* 18,1 (1948).
 53. H. Knudsen, in *Physics of Electronic and Atomic Collisions*, edited by S. Datz, p. 657, North-Holland Publishing Company, 1982.
 54. M. Kimura and N. F. Lane, *Adv. At. Mol. Opt. Phys.* 26, 79 (1989).
 55. R. McCarroll and A. Salin, *J. Phys. B: At. Mol. Opt. Phys.* 1, 163 (1968).
 56. A. Dubois, S. E. Nielsen, and J. P. Hansen, *J. Phys. B: At. Mol. Opt. Phys.* 26, 705 (1993).
 57. W. Fritsch and C. D. Lin, *Phys. Rev. A* 54, 4931 (1996).
 58. J. Schweinzer, D. Wutte, and HP. Winter, *J. Phys. B: At. Mol. Opt. Phys.* 27, 137 (1994).
 59. H. J. Liidde, A. Henne, T. Kirchner, and R. M. Dreizler, *J. Phys. B: At. Mol. Opt. Phys.* 29,4423 (1996).